Transverse "Bouncing" of Polarized Laser Beams in Sodium Vapor

R. Holzner and P. Eschle
Physik-Institut der Universität Zürich, Winterthurerstrasse 190, CH-8057 Zürich, Switzerland

A. W. McCord and D. M. Warrington
Physics Department, University of Otago, Dunedin, New Zealand
(Received 4 June 1992)

Two intersecting laser beams of orthogonal circular polarization near resonant to the homogeneously broadened $D1$ transition of Na vapor were observed to deflect each other upon contact. The experimental results are in good agreement with calculations based on a model which includes diffraction and a *local* nonlinear atomic susceptibility which fully takes into account saturation and optical pumping effects. The contact deflection (or "bouncing") was also observed when both beams were tuned to the atomic resonance frequency.

PACS numbers: 42.25.Bs, 32.80.Bx, 42.60.−v, 78.70.−g

Although there has been considerable interest in the role of transverse diffractive effects in optical instabilities and in the formation of optical spatial patterns [1], relatively little attention has been given to the propagation of arbitrarily polarized light. Recent calculations of cw laser light propagation in multistate atomic vapors, which include diffraction, saturation, and optical-pumping-induced polarization effects, have shown that the coupling between the polarization components of the electric field vector can give rise to surprising diffractive beam reshaping during propagation. For example, elliptically polarized Gaussian beams can break up into pure circularly polarized rings [2,3] and linearly polarized beams can break cylindrical symmetry and form multiple beams or filaments of pure circular polarization [4].

This paper presents a theoretical prediction and experimental confirmation of a localized spatial interaction between two polarized laser beams in an alkali vapor. Our theoretical calculation predicts that two laser beams of orthogonal circular polarization, which intersect at a small angle in a vapor of homogeneously broadened four-state atoms undergoing a $J=\frac{1}{2}\rightarrow J=\frac{1}{2}$ transition, will mutually deflect each other upon contact. We report in detail on our experimental verification of this effect using the $D1$ transition in sodium vapor.

The theoretical model assumes homogeneous broadening and an entirely *local* nonlinear response of the atoms. That is, the complex susceptibility at a point in the medium is determined by the electric field vector at that point and the simulation, in effect, assumes the atoms to be stationary. To approximately realize these conditions experimentally we use a mixture of sodium vapor with 250 Torr of argon buffer gas which provides both homogeneous broadening and spatial confinement of the sodium atoms via Ar-Na collisions.

In our theoretical calculation we assume that the two circularly polarized input beams of equal waist w_0 and angular frequency ω_l are coplanar and enter the nonlinear medium at $z=0$. The wave vectors of the input beams $\mathbf{k}_1$ and $\mathbf{k}_2$ lie in the plane defined by $y=0$ and make angles $\pm\theta$ with respect to the z axis. Dimensionless spatial coordinates $(\bar{x},\bar{y},\bar{z})$ are defined as $(x/w_0, y/w_0, z/4z_R)$, where $z_R=\frac{1}{2}kw_0^2$ is the free-space Rayleigh length of a beam of waist w_0, and where $k=\omega_l/c=|\mathbf{k}_1|=|\mathbf{k}_2|$. If the "collision angle" 2θ between the input beams is sufficiently small, the propagation of the circular polarization components $E_\pm$ of the electric field, expressed in saturation units, may be described by the paraxial Maxwell-Bloch equations [2]:

$$\frac{\partial E_+}{\partial\bar{z}}=i\left[\frac{\partial^2E_+}{\partial\bar{x}^2}+\frac{\partial^2E_+}{\partial\bar{y}^2}\right]-2F\frac{(1+i\Delta)E_+}{1+8I_++2(\beta-2)(I_+-I_-)/(1+4\beta I_-)}, \tag{1}$$

$$\frac{\partial E_-}{\partial\bar{z}}=i\left[\frac{\partial^2E_-}{\partial\bar{x}^2}+\frac{\partial^2E_-}{\partial\bar{y}^2}\right]-2F\frac{(1+i\Delta)E_-}{1+8I_-+2(\beta-2)(I_--I_+)/(1+4\beta I_+)}. \tag{2}$$

The relative importance of the absorptive and dispersive action of the medium compared to the diffractive Laplacian terms is parametrized by the quantity $F=\alpha_0z_R/(1+\Delta^2)$, where α_0 is the weak field resonant absorption coefficient. The parameter $\Delta=(\omega_l-\omega_0)/\Gamma_{lu}$ is the detuning of the input beams from the atomic resonance frequency ω_0 divided by the full width at half maximum of the homogeneously broadened transition. The "optical pumping parameter" $\beta=\gamma/\Gamma_u+\gamma/\Gamma_l-\gamma^2/3\Gamma_l\Gamma_u$ is defined [2] in terms of the natural decay rate γ and the orientation decay rates in the lower (Γ_l) and upper (Γ_u) atomic levels. For the conditions of our experiment we have $\Gamma_{lu}=1.0\times10^{10}\ \mathrm{s}^{-1}$, $\Gamma_u=\gamma=6.25\times10^7\ \mathrm{s}^{-1}$, and Γ_l is estimated from the average diffusion time of Na atoms through the laser beam to be $1.6\times10^4\ \mathrm{s}^{-1}$. Equations (1) and (2) contain dimensionless effective intensities defined by $I_\pm=[E_\pm^*(x,y,z)E_\pm(x,y,z)]/(1+\Delta^2)$ and

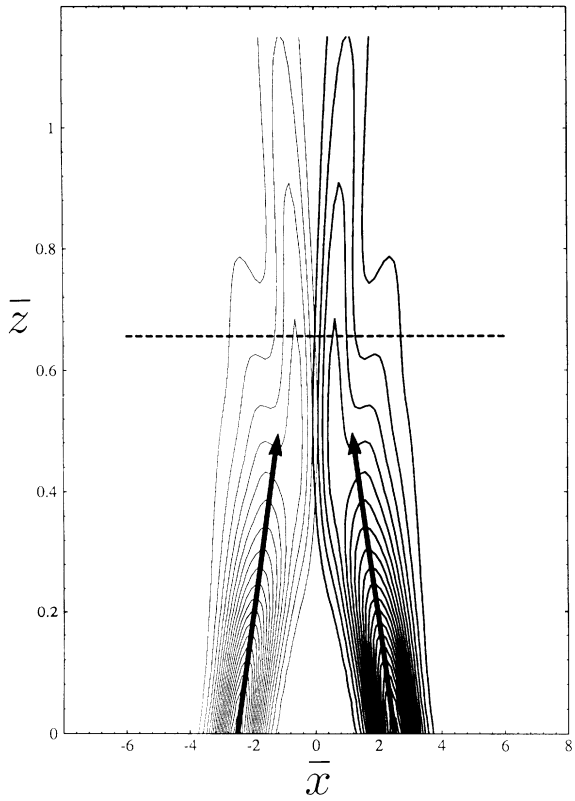

FIG. 1. Calculated isointensity contours of I_+ (thick) and I_- (thin) circularly polarized laser beams during propagation in the positive z direction, using parameter values determined for our experimental conditions. The initial **k** vector of each beam (thick arrow) is tilted so that they would intersect at $\bar{z}=0.94$. The theoretical parameters are $F=5$, $I_{\pm\max}=2.5$, $\beta=2650$, and $\Delta=0.82$. The laboratory intersection angle 2θ is equal to 5 mrad. The dashed line represents the $\bar{z}$ depth of the cross sections shown in Fig. 5. The contour spacing is $\frac{1}{8}$.

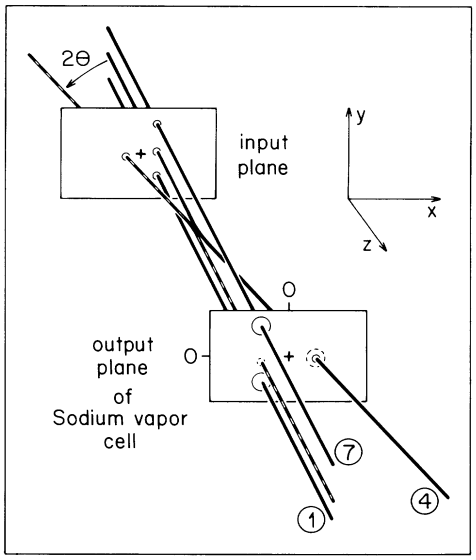

FIG. 2. Schematics of "beam bouncing" experiment: The three solid lines are successive positions of a circularly polarized beam as it is swept vertically through a stationary beam (dashed line) of orthogonal polarization. In positions 1 and 7 the beams are not coplanar and propagate without interaction. In position 4 both beams intersect and mutual deflection occurs.

have been numerically integrated using a split-step fast-Fourier method incorporating the implicit solution of the nonlinear equations.

Figure 1 shows the calculated spatial evolution of the intensities of the polarized laser beams recorded in the $y=0$ plane within the nonlinear medium as the beams propagate paraxially in the z direction. As the beams begin to overlap, they are clearly mutually deflected.

For detunings above resonance an intuitive explanation of the basic mechanism can be given as follows: The atoms within each beam are optically pumped into the atomic state which does not absorb light of that polarization. However, this state interacts strongly with light of the orthogonal polarization. Where the beams begin to overlap, each is entering a steep gradient of refractive index which mutually deflects each beam. A transverse modulational pattern in the interaction region can be clearly seen in Fig. 1 as a developing "side lobe." This modulation can be interpreted in terms of interference between the incoming and outgoing parts of each beam just as in reflection from a mirror at grazing incidence.

The geometrical arrangement of the laser beam paths for the beam bouncing experiment is shown schematically in Fig. 2. One beam is held stationary while the other beam is swept vertically through it. For positions 1 and 7 the centers of the two beams in our experiment are separated in the vertical direction by about 0.6 mm and no interaction is observed—each beam experiences self-trapping and propagates without deviation. However, for position 4 the input beams are coplanar and therefore intersect. In this case we find the interaction is sufficient to completely reflect each beam. At intermediate positions a partial deflection combined with increased absorption takes place.

The overall experimental setup is shown in Fig. 3. A Coherent 699-29 cw ring dye laser is tuned close to the sodium $D1$ transition. An attenuator consisting of a $\lambda/2$ plate between two high-quality linear polarizers gives adjustment of the intensity with minimum beam deviation. Two beams with orthogonal linear polarizations are obtained by a Rochon polarizing calcite prism; the polarization rotator allows the intensities of the two beams to be balanced. An arrangement of three mirrors and a beam splitter is used to achieve small separations and angles between the two beams. The beam passing through the beam splitter remains stationary throughout the experiment, while the beam reflected from the surface is adjusted horizontally for intersection angle and vertically for sweeping through the stationary beam. When the distance between the beam splitter and the following lens is

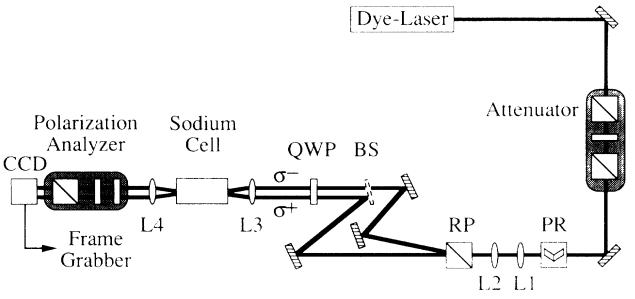

FIG. 3. Experimental setup. Attenuator, consisting of a half wave plate between two polarizers; PR, polarization rotator; L1–L4, lenses; RP, Rochon type calcite prism; BS, beam splitter; QWP, quarter wave plate; polarization analyzer, consisting of a quarter wave plate, a half wave plate, and a polarizer; CCD, CCD video camera.

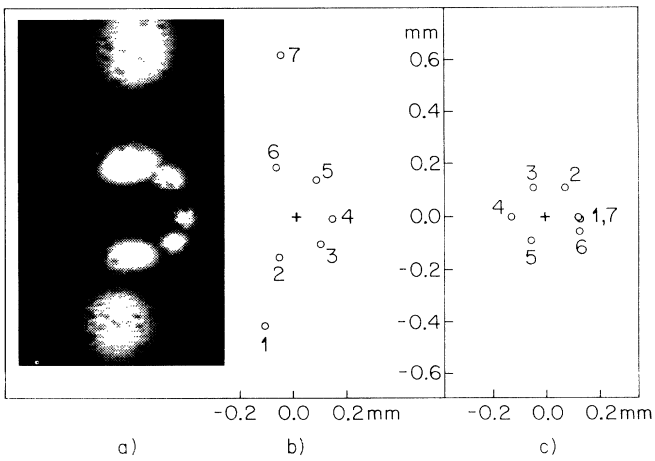

FIG. 4. "Beam bouncing" demonstrated. (a) Superposition of seven CCD camera images of the swept beam spot at the cell output plane for input beam positions 1–7; (b) spot centers of the swept beam; (c) spot centers of the stationary beam. The "+" marks the projection of the beam intersection point ($x=0, y=0$). At position 4 the beam waist separation is 0.5 mm at the input plane of the cell. The angle 2θ of a few mrad between the incident beams is approximately equal to the angle between the emerging beams.

equal to the lens focal length, the beam direction remains constant during this vertical sweep. After the $\lambda/4$ plate the beams have orthogonal circular polarizations. The three lenses produce beam waists of 50 μm at the input window of the sodium vapor cell, and the power in each beam is typically 4 mW. The Pyrex cell is 6.5 cm long and 2 cm in diameter, with 2-mm-thick, $\lambda/10$ flat windows which are tilted by an angle of about 5° to avoid etalon effects. The cell contains argon buffer gas at a pressure of 250 Torr, and is heated to 207 °C in a small oven. The sodium atom density (3.7×10^{18} m^{-3}) is obtained from the absorption profile for a low intensity beam, which is fitted to a line-shape function based on four Voigt profiles at the known hyperfine separations. The oven heating wires are arranged for minimum dc magnetic field, and a set of three orthogonal square Helmholtz coils is used around the cell and oven to cancel any local dc magnetic field and to apply a small field (typically 200 mG) parallel to the light beams to ensure that the longitudinal component dominates any residual transverse component. The lens following the cell images the output window with ×2 magnification onto the charge-coupled-device (CCD) array of a Pulnix TM-765 camera. A $\lambda/4$ plate, a $\lambda/2$ plate, and a high-quality linear polarizer between the imaging lens and the camera allow for polarization analysis. The signal from the camera is digitized by a Data Translation DT2853 frame grabber to produce a 512 by 512 pixel frame with ultimate resolution 5 μm at the output window.

During the experiment, the vertical position of the swept beam was adjusted manually, and, for each position, each beam was recorded separately by altering the polarization analyzer. Figure 4(a) shows the spot of the swept beam at the cell output window for seven input positions superimposed onto a single photograph. In Figs. 4(b) and 4(c) the spot centers of both the swept and stationary beams for positions 1 through 7 are indicated. In the closer positions 3,4,5 the two spots move approximately in a circle at opposite ends of a diameter which rotates about the center. A photograph of the stationary beam spots, analogous to Fig. 4(a), is not shown since the larger spots at positions 1,2,6,7 would cover the smaller spots at positions 3,4,5.

For the results presented here the laser was tuned slightly above resonance (by 1.3 GHz) but we observed beam bouncing also at lower atomic density with the laser on resonance (i.e., at the frequency for which maximum absorption is observed at low input intensities). Resonant beam bouncing was also found in our simulations. The explanation of bouncing on resonance is more subtle since the refractive index experienced by each beam has no spatial variation. However, where the beams meet in the $x=0$ plane, the equal amplitudes of left and right circularly polarized radiation constitute linearly polarized light which cannot optically pump the atoms and both beams therefore suffer strong absorption in this plane. The consequent sudden amplitude dropoff experienced by each beam as it approaches the $x=0$ plane is similar to the boundary condition encountered by a single beam approaching a metallic mirror surface and the beam is reflected.

The modulational pattern evident in the simulation of Fig. 1 can be observed experimentally by moving the horizontal position of the swept beam so that the intersection point is closer to the output window of the cell. Figure 5 shows the experimentally recorded beam cross section in this region, with a contour plot of its intensity and the corresponding cross section from the theoretical simulation.

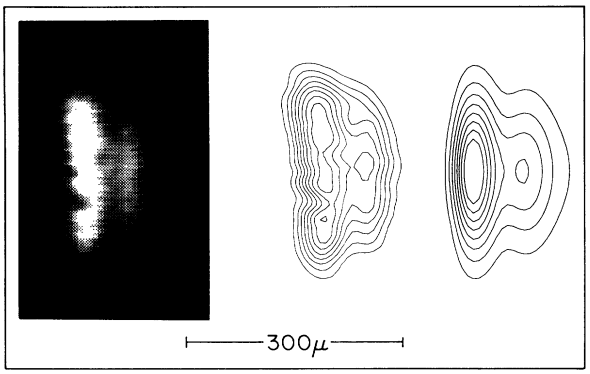

FIG. 5. Comparison of experimental and theoretical profiles in the region of beam intersection: (a) CCD camera image of the cross section of the swept beam at position 4, showing the riblike modulation pattern (the stationary beam has a structure which is a mirror image of that displayed here). (b) Contour plot of (a). (c) Corresponding theoretical simulation using parameters as in Fig. 1. The cross sections displayed here are recorded at a distance into the medium indicated by the dashed line in Fig. 1.

Tam and Happer [5] have reported noncontact long-range interactions between laser beams tuned to the high-frequency side of the $D1$ transition. The observation was explained in terms of the diffusion of spin polarized atoms between the beams. In their case the characteristic atom diffusion length was much greater than the characteristic laser beam radius and the spatial effect they observed was dominated by diffusion gradients.

By adding an inert buffer gas to spatially localize the atoms we have been able to operate in the diffraction-dominated regime in which the beams come into contact and mutually waveguide each other via *local* optical pumping of the atoms. The much sharper refractive index gradients achievable in this regime result in the characteristic modulational patterns formed as each beam is partially reflected back onto itself. We have also reported the surprising result that on resonance, where there is no nonlinear refractive index at all, nonlinear absorption alone is capable of producing beam bouncing by inducing an effective mirrorlike boundary condition.

[1] Special issue on Transverse Effects in Nonlinear-Optical Systems, J. Opt. Soc. Am. B **7** (1990).
[2] A. W. McCord and R. J. Ballagh, J. Opt. Soc. Am. B **7**, 73–83 (1990).
[3] R. J. Ballagh and A. W. McCord, Int. J. Nonlin. Opt. Phys. **1**, 393–420 (1992).
[4] A. W. McCord, J. Opt. Soc. Am. B **8**, 2013–2019 (1991).
[5] A. C. Tam and W. Happer. Phys. Rev. Lett. **38**, 278–282 (1977).

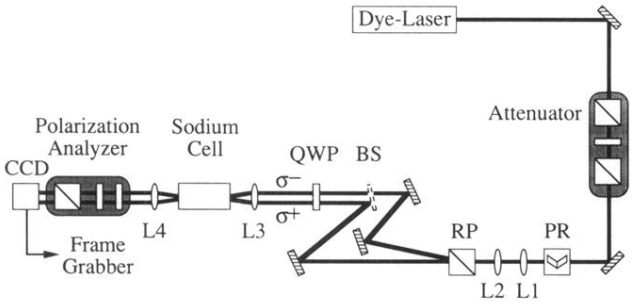

FIG. 3. Experimental setup. Attenuator, consisting of a half wave plate between two polarizers; PR, polarization rotator; L1–L4, lenses; RP, Rochon type calcite prism; BS, beam splitter; QWP, quarter wave plate; polarization analyzer, consisting of a quarter wave plate, a half wave plate, and a polarizer; CCD, CCD video camera.

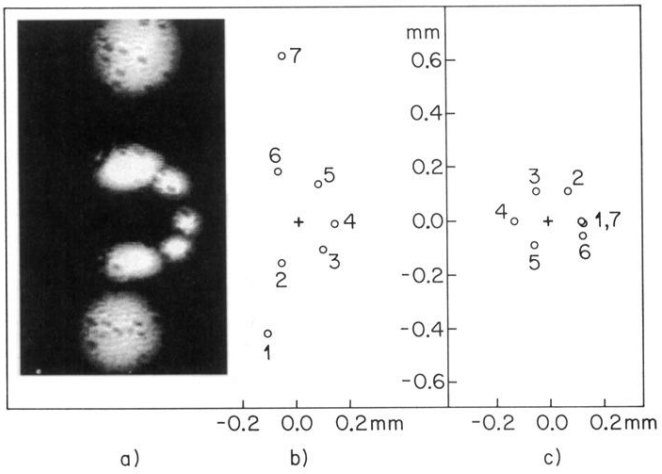

FIG. 4. "Beam bouncing" demonstrated. (a) Superposition of seven CCD camera images of the swept beam spot at the cell output plane for input beam positions 1–7; (b) spot centers of the swept beam; (c) spot centers of the stationary beam. The "+" marks the projection of the beam intersection point ($x=0, y=0$). At position 4 the beam waist separation is 0.5 mm at the input plane of the cell. The angle 2θ of a few mrad between the incident beams is approximately equal to the angle between the emerging beams.

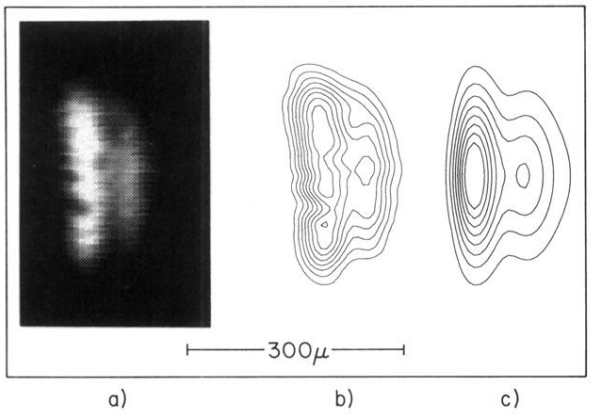

FIG. 5. Comparison of experimental and theoretical profiles in the region of beam intersection: (a) CCD camera image of the cross section of the swept beam at position 4, showing the riblike modulation pattern (the stationary beam has a structure which is a mirror image of that displayed here). (b) Contour plot of (a). (c) Corresponding theoretical simulation using parameters as in Fig. 1. The cross sections displayed here are recorded at a distance into the medium indicated by the dashed line in Fig. 1.